

Superconducting properties of well-shaped MgB_2 single crystal

Kijoon H. P. Kim,¹ Jae-Hyuk Choi,¹ C. U. Jung,¹ P. Chowdhury,¹ Min-Seok Park,¹ Heon-Jung Kim,¹ J. Y. Kim,¹ Zhonglian Du,¹ Eun-Mi Choi,¹ Mun-Seog Kim,¹ W. N. Kang,¹ Sung-Ik Lee,^{1*} Gun Yong Sung,² and Jeong Yong Lee³

¹*National Creative Research Initiative Center for Superconductivity and
Department of Physics, Pohang University of Science and Technology, Pohang
790-784, Republic of Korea*

²*Telecommunications Basic Research Laboratory, Electronics and
Telecommunications Research Institute, Taejeon 305-350, Republic of Korea*

³*Department of Material Science and Engineering, Korea Advanced
Institute of Science and Technology, Taejeon 305-701, Republic of Korea
(April 26, 2024)*

We report measurements of the transport and the magnetic properties of high-quality, sub-millimeter-sized MgB_2 single crystals with clear hexagonal-plate shapes. The low-field magnetization and the magnetic hysteresis curves show the vortex pinning of these crystals to be very weak. The Debye temperature of $\Theta_D \sim 1100$ K, obtained from the zero-field resistance curve, suggests that the normal-state transport properties are dominated by electron-phonon interactions. The resistivity ratio between 40 K and 300 K was about 5, and the upper critical field anisotropy ratio was 3 ± 0.2 at temperatures around 32 K.

The recent discovery [1] of binary metallic MgB_2 with a superconducting transition temperature of 39 K has attracted great scientific [2–19] and applicatory interests [20–25]. The negligibly small effect of its grain boundary on the supercurrent [20–22] suggests increased potential for device applications. Also, vortex pinning, and thus the critical current, is vastly enhanced in c -axis-oriented thin films [23,24] or in the bulk when disorder is induced by proton irradiation [25]. Aside from the basic properties such as the charge carrier type [2], many scientific issues, such as the order parameter symmetry [3,4], the upper critical field anisotropy ratio [5,12], $\gamma = H_{c2}^{ab}/H_{c2}^c$, the Θ_D [26], and the transport properties of the normal-state are still controversial.

Especially, the anisotropy is an important property because it significantly affects the electronic and the magnetic properties, such as the pinning mechanism of this material. The anisotropy ratio has been reported to be 6 - 9 for the powder. This range of values was estimated by using conduction electron spin resonance [27]. The values for aligned crystallites [5], c -axis oriented films [12,28], and single crystals grown by different techniques [15,16] are reported as 1.7, 1.3 - 2, and 2.6 - 2.7, respectively.

The high superconducting transition temperature in MgB_2 has been considered to be due to strong electron-phonon coupling [17,29,30]. Thus it is important to know whether the normal-state transport properties can be described by a simple electron-phonon interaction, or electron correlation has to be taken into account.

Other issues are the temperature dependence of the normal-state resistivity and the value of the residual resistivity ratio (RRR), $\rho(300 \text{ K})/\rho(40 \text{ K})$. The RRR was reported to vary from 2 to 25 depending on the prepara-

tion conditions [6–10,23,24], and the magnetoresistance (MR) at normal-state was reported to vary from 1% to 60% [8,10–12], with a rough correlation between higher RRR and higher MR values. These issues can be clarified if these quantities are measured in very clean single crystals. Such results will also help to construct a theoretical formulation [13].

In this Letter, we report the transport and the magnetic properties of very clean MgB_2 single crystals. The crystals were found to have well-shaped hexagonal plates with an a -axis lattice constant of 3.09 Å. The superconducting transition occurred at 38 K with a sharp transition width of 0.3 K. The low-field magnetization and the magnetic hysteresis curve showed the vortex pinning to be very weak, which supported our crystals being very clean. The γ and the Θ_D were obtained by directly measuring the temperature- and field-dependence of resistance for different field directions.

MgB_2 bulk pieces [8,14] were heat treated in a Mg flux inside a Nb tube, which was sealed in an inert gas atmosphere by using an arc furnace. Then, the Nb tube was put inside a quartz ampoule, which was sealed in vacuum. The quartz tube was heated for one hour at 1050 °C, then very slowly cooled to 700 °C for five to fifteen days, and quenched to room temperature. For all measurements, the single crystals were separated from the resultant matrix using a mechanical method. Details of growth will be found elsewhere [31]. The crystal images were observed using a polarizing optical microscope and a field-emission scanning electron microscope (SEM). Structural analysis was carried out using a high-resolution transmission electron microscope (HRTEM). The magnetization curves were measured by using a SQUID magnetometer.

Resistivity measurements were performed using the standard dc 4-probe method.

Figure 1(a) shows a typical SEM image for a MgB_2 single crystal. Most of the crystals were found to have hexagonal-plate forms with typical edge angles of 120 degrees and very flat surfaces, which were very shiny while observed using a polarizing optical microscope. The crystals were about $20 \sim 60 \mu\text{m}$ in diagonal length and $2 \sim 6 \mu\text{m}$ in thickness. A recent study [6] showed that [001] twist grain boundaries, formed by rotations along the c -axis (typically by about 4 degrees), were the major grain boundaries in polycrystalline MgB_2 , which could be attributed to the weaker Mg-B bonding [6]. HRTEM and SEM studies showed no grain boundaries in our crystals. Figure 1(b) shows a magnified view of the upper corner of the crystal shown in Fig. 1(a). The smooth surfaces and the sharp edges in this figure confirm that our small crystals had the least probability of having mosaic aggregates of nanocrystals either along the ab -plane or along the c -axis; thus, we had a better chance to study their intrinsic properties with the help of a micro-fabrication technique.

To measure the temperature and the field dependencies of the in-plane resistivity of the crystal, we fabricated four electrical metal leads (bright area) on the top surface of the crystal, as shown in Fig. 1(c). For lithography, selected MgB_2 single crystals were fixed on oxidized Si substrate by holding their hexagonal edges using a negative photoresist (OMR-83, TOK Co. Ltd.) as glue. They were then soft-baked. After the surfaces of the samples were cleaned by using Ar-ion milling with a beam voltage of 350 V and a beam current of 0.2 mA/cm^2 , four electrical pads were patterned using a positive photoresist (AZ 7210, Clariant Industries Ltd.). Three metal layers, a 100 nm-thick Ti film, a 1000 nm-thick Ag film, and a 100 nm-thick Au film, were deposited in sequence after another ion milling treatment. The contact resistances were less than 2Ω , and the approximate distance between the voltage pads was about $7 \mu\text{m}$. The bias current for the resistance measurement was $0.1 \sim 0.2 \text{ mA}$, which, judging from the current-voltage characteristics, was in the ohmic range.

To confirm the structure of the MgB_2 phase, we took a plane-view HRTEM image, as shown in Fig. 2. From this high-resolution image, the a -axis lattice parameter was found to be $3.09 \pm 0.06 \text{ \AA}$, which was consistent with the value determined from X-ray powder diffractometry performed on polycrystalline samples [1]. Figure 2(b) shows the electron diffraction pattern in a selected area for a beam direction of [001]. This result clearly indicates that this crystal has the hexagonal structure of MgB_2 .

Figure 3(a) shows the in-plane resistance as a function of temperature. A superconducting transition appeared near 38 K, and the transition width was 0.3 K based on the 10 to 90% drop of the resistance curve at zero field. The RRR was about 5, which was confirmed for our sev-

eral crystals and was consistent with the values for single crystals recently reported [15,16]. This is quite different from the reported values for polycrystals [6–10] and high-quality thin films [23,24]. Extrinsic effects, such as impurities or grain boundaries, might be the origins of these diverse observations [6,7]. The c -axis resistivity of single crystals should be studied for more understanding; however, this is still challenging yet due to the thickness of our crystals.

The solid line in Fig. 3 is a fitting curve obtained using the Bloch-Grüneisen formula [26] in the normal state: $R(T) = R_0 + R_{\text{ph}}(T)$ where R_0 is the temperature-independent residual part and $R_{\text{ph}}(T)$ the phonon scattering contribution given by the relation:

$$R_{\text{ph}}(T) = R_1 \left(\frac{T}{\Theta_D} \right)^m \int_0^{\Theta_D/T} \frac{z^m dz}{(1 - e^{-z})(e^z - 1)}, \quad (1)$$

with R_1 being a proportionality constant. The best fit to our data was obtained with $m = 3$ and $\Theta_D \sim 1100 \text{ K}$. This values of the Θ_D is comparable to those (746 - 1050 K) previously reported based on the specific heat and resistivity measurements on polycrystalline samples [17,18,32–34]. This result suggests that the normal-state transport properties are well described by an electron-phonon interaction without taking an electron-electron interaction into account.

The two insets of Fig. 3(a) show the field dependencies of the in-plane resistances while maintaining the applied field perpendicular to the current path. The magnetoresistance at 5 T was found to change with the direction of the field with respect to the crystal axis. For fields parallel to the ab -plane ($H \parallel ab$) and to the c -axis ($H \parallel c$), the magnetoresistances at 40 K were $\lesssim 3\%$ and $\sim 20\%$, respectively, which was confirmed for our several crystals. To determine the temperature dependence of the upper critical field H_{c2} , we measured the resistance at several fields up to 5 T. From these curves, we obtained $H_{c2}(T)$ as shown in Fig. 3(b), where a 10% drop of the resistance was adopted to determine $T_c(H)$. The ratio of the upper critical field for $H \parallel ab$ to that for $H \parallel c$ was 3 ± 0.2 at temperatures around 32 K. This value is consistent with those for single crystals grown by different techniques [15,16].

To confirm the bulk properties of the superconductivity, we measured the low-field magnetization curve $M(T)$ and the magnetic hysteresis curve $M(H)$. Since the volume of one crystal is rather small, we fixed about a hundred single crystals on a Si substrate with their c -axes aligned perpendicular to the substrate surface, which is similar to the method used by others [5]. To avoid spurious signals from matrix, we used an optical microscope and a sample-handling device equipped with a precision xyz -stage and a micro-tip to collect large single crystals one by one.

Figure 4(a) shows the $M(T)$ curves measured at 20 Oe in the zero-field-cooling (ZFC) and the field-cooling

(FC) modes. The T_c onset was observed to be ~ 38 K, which is consistent with the value obtained from the resistance measurement. The difference between the FC and the ZFC data is quite small compared to those of polycrystalline samples [8,14] or single crystals prepared at higher temperature [16], suggesting that pinning is very weak in our single crystals. The different values of $M(T)$ for different field directions give a demagnetization factor $D \gtrsim 0.6$, which is consistent with the value calculated by considering the shape of the crystals.

Figure 4(b) shows the magnetic hysteresis curves $M(H)$ at 5 K. The $M(H)$ data show a negligible paramagnetic background. The different slopes of the $M(H)$ curves at low starting fields ($H < 300$ Oe) for different field directions are due to the demagnetization factors being different. The difference between the values of $M(H)$ for the increasing and the decreasing field branches is rather small, which also shows that bulk pinning is very small and, thus, supports our crystals being very clean. The results in Figs. 4(a) and 4(b) indicate that the strong bulk pinning reported for polycrystals [19] and thin films [23,24] is due to extrinsic pinning sites, such as grain boundaries and crystallographic defects.

In summary, we report the transport and the magnetic properties for high-quality MgB_2 single crystals. A superconducting transition occurred at 38 K with a sharp transition width of 0.3 K. The low-field magnetization and the magnetic hysteresis curve showed the vortex pinning to be very weak. From the resistance measurement, a Θ_D of ~ 1100 K was obtained using the Bloch-Grüneisen formula, which suggests that the normal-state transport properties are dominated by an electron-phonon interaction rather than by an electron-electron interaction. A RRR of 5 and a γ of 3 ± 0.2 at temperatures around 32 K, were obtained.

This work is supported by the Ministry of Science and Technology of Korea through the Creative Research Initiative Program. This work was partially supported by the National Research Laboratory Program through the Korea Institute of Science and Technology Evaluation and Planning. We acknowledge Do Hyun Lim and Taek-Jung Shin at Iljin Diamond Co., Ltd., for their help.

- mat/0103287 (2001).
- [6] Y. Zhu *et al.*, cond-mat/0105311 (2001).
 - [7] Y. Y. Xue *et al.*, cond-mat/0105478 (2001).
 - [8] C. U. Jung *et al.*, Physica C **353**, 162 (2001).
 - [9] P. C. Canfield *et al.*, Phys. Rev. Lett. **86**, 2423 (2001).
 - [10] D. K. Finnemore, J. E. Ostenson, S. L. Bud'ko, G. Laperot, and P. C. Canfield, Phys. Rev. Lett. **86**, 2420 (2001).
 - [11] S. L. Bud'ko *et al.*, Phys. Rev. B **63**, 220503 (2001).
 - [12] M. H. Jung *et al.*, Chem. Phys. Lett. (in press), cond-mat/0106146 (2001).
 - [13] Y. Kong, O. V. Dolgov, O. Jepsen, and O. K. Andersen, Phys. Rev. B **64**, 020501 (2001).
 - [14] C. U. Jung *et al.*, Appl. Phys. Lett. **78**, 4157 (2001).
 - [15] M. Xu *et al.*, cond-mat/0105271 (2001).
 - [16] S. Lee *et al.*, cond-mat/0105545 (2001).
 - [17] S. L. Bud'ko *et al.*, Phys. Rev. Lett. **86**, 1877 (2001).
 - [18] Ch. Wälti *et al.*, cond-mat/0102522 (2001).
 - [19] Mun-Seog Kim *et al.*, Phys. Rev. B **64**, 12511 (2001).
 - [20] Y. Bugoslavsky, G. K. Perkins, X. Qi, L. F. Cohen, and A. D. Caplin, Nature **410**, 563 (2001).
 - [21] D. C. Labaestier *et al.*, Nature **410**, 186 (2001).
 - [22] Kijoon H. P. Kim *et al.*, cond-mat/0103176 (2001).
 - [23] W. N. Kang, H.-J. Kim, E.-M. Choi, C. U. Jung, and S.-I. Lee, Science **292**, 1523 (2001).
 - [24] C. B. Eom *et al.*, Nature **411**, 558 (2001).
 - [25] Y. Bugoslavsky *et al.*, Nature **411**, 561 (2001).
 - [26] Charles P. Poole, Jr. Handbook of Superconductivity, 31-32 (Academic Press, Florida, 2000).
 - [27] F. Simon *et al.*, cond-mat/0104557 (2001).
 - [28] S. Patnaik *et al.*, cond-mat/0104562 (2001).
 - [29] J. Kortus *et al.*, Phys. Rev. Lett. **86**, 4656 (2001).
 - [30] M. Monteverde *et al.*, Science **292**, 75 (2001).
 - [31] C. U. Jung *et al.*, (unpublished) or Jae-Hyuk Choi, Ph. D. thesis paper(2001), Dept. Phys., Postech, Korea.
 - [32] R. K. Kremer, B. J. Gibson, and K. Ahn, cond-mat/0102432 (2001).
 - [33] F. Bouquet *et al.*, cond-mat/0104206 (2001).
 - [34] M. Putti *et al.*, cond-mat/0106344 (2001).

* Corresponding author: silee@postech.ac.kr.

- [1] J. Nagamatsu, N. Nakagawa, T. Muranaka, Y. Zenitani, and J. Akimitsu, Nature **410**, 63 (2001).
- [2] W. N. Kang *et al.*, cond-mat/0102313 (2001).
- [3] C.-T. Chen *et al.*, cond-mat/0104285 (2001).
- [4] G. Karapetrov, M. Iavarone, W. K. Kwok, G. W. Crabtree, and D. G. Hinks, Phys. Rev. Lett. **86**, 4374 (2001).
- [5] O. F. de Lima, R. A. Ribeiro, M. A. Avila, C. A. Cardoso, and A. A. Coelho, Phys. Rev. Lett. (in press), cond-

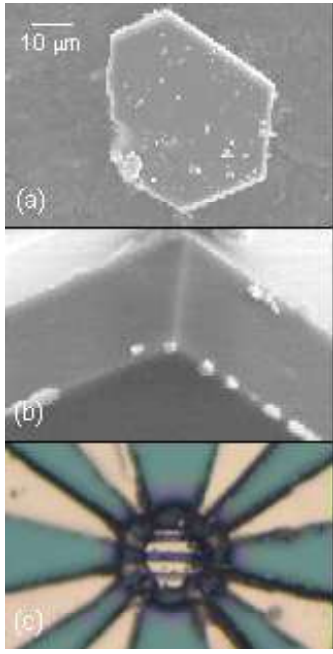


FIG. 1. (a) SEM image of a hexagonal, thin plate with a size of about $50\ \mu\text{m}$, (b) A magnified view of the upper corner of the crystal shows smooth surfaces and sharp edges. The white spots at the edge were stuck weakly on the crystal surface and were about $100\ \text{nm}$ in diameter. (c) Optical microscope image of the 4-probe contact leads which were made on a single crystal by using a photolithography technique.

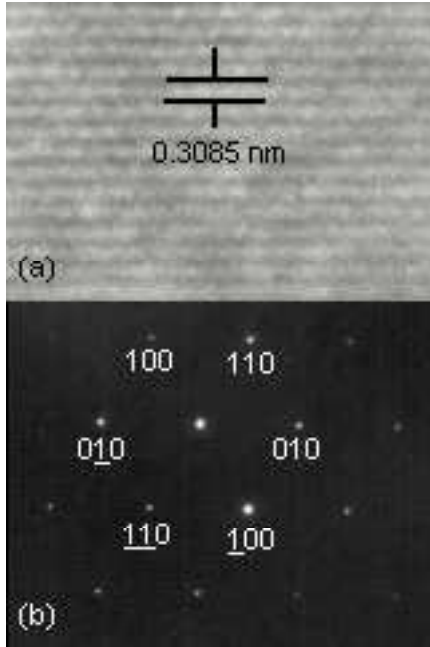


FIG. 2. (a) HRTEM image of a MgB_2 single crystal and (b) selected area electron diffraction pattern for a beam direction of $[001]$ in the hexagonal structure.

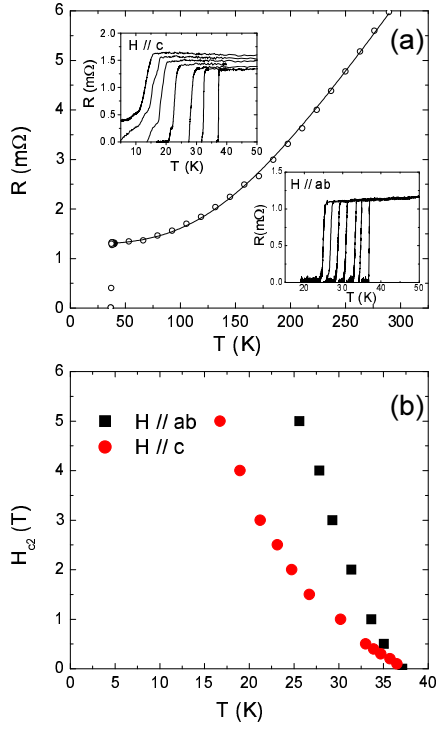


FIG. 3. (a) Resistance of a MgB_2 single crystal as a function of temperature for magnetic fields from 0 to 5 T. The residual resistivity ratio was about 5. The insets show the resistance for fields perpendicular and parallel to the crystal c -axis at 0.0, 0.5, 1.0, 2.0, 3.0, 4.0, and 5 T. (b) The upper critical field determined from a 10% drop of the resistance as a function of temperature for several fields up to $H = 5$ T.

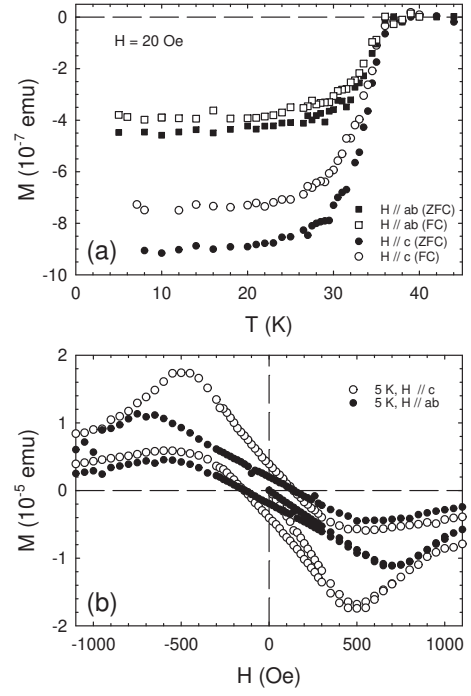


FIG. 4. (a) Low-field $M(T)$ curves of MgB_2 single crystals measured at 20 Oe for fields parallel and perpendicular to the c -axis. (b) $M(H)$ hysteresis curves measured at 5 K.